JACS
JOURNAL OF THE AMERICAN CHEMICAL SOCIETY
Article
pubs.acs.org/JACS

Testing the Polynuclear Hypothesis: Multielectron Reduction of Small Molecules by Triiron Reaction Sites

Tamara M. Powers and Theodore A. Betley*

Department of Chemistry and Chemical Biology, Harvard University, 12 Oxford Street, Cambridge, Massachusetts 02138, United States

Supporting Information

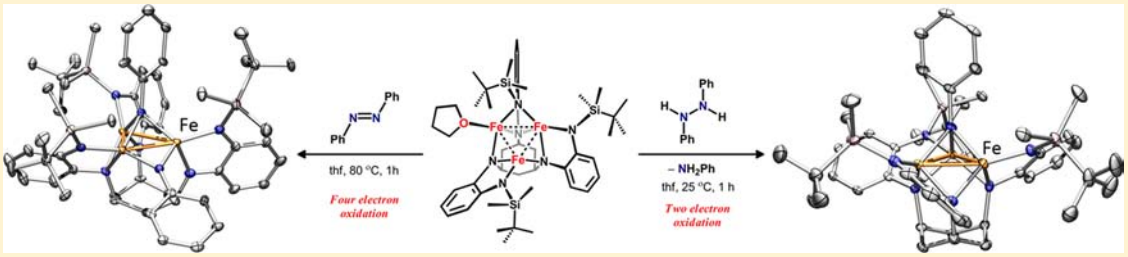

ABSTRACT: High-spin trinuclear iron complex (^{tbs}L)Fe$_3$(thf) ([^{tbs}L]$^{6-}$ = [1,3,5-C$_6$H$_9$(NC$_6$H$_4$-*o*-NSi^{t}BuMe$_2$)$_3$]$^{6-}$) (S = 6) facilitates 2 and 4e$^-$ reduction of N$_x$H$_y$ type substrates to yield imido and nitrido products. Reaction of hydrazine or phenylhydrazine with (^{tbs}L)Fe$_3$(thf) yields triiron μ^3-imido cluster (^{tbs}L)Fe$_3$(μ^3-NH) and ammonia or aniline, respectively. (^{tbs}L)Fe$_3$(μ^3-NH) has a similar zero-field ^{57}Fe Mössbauer spectrum compared to previously reported [(^{tbs}L)Fe$_3$(μ^3-N)]NBu$_4$, and can be directly synthesized by protonation of the anionic triiron nitrido with lutidinium tetraphenylborate. Deprotonation of the triiron parent imido (^{tbs}L)Fe$_3$(μ^3-NH) with lithium bis(trimethylsilyl)amide results in regeneration of the triiron nitrido complex capped with a thf-solvated Li cation [(^{tbs}L)Fe$_3$(μ^3-N)]Li(thf)$_3$. The lithium capped nitrido, structurally similar to the pseudo C_3-symmetric triiron nitride with a tetrabutylammonium countercation, is rigorously C_3-symmetric featuring intracore distances of Fe−Fe 2.4802(5) Å, Fe−N$_{(nitride)}$ 1.877(2) Å, and N$_{(nitride)}$−Li 1.990(6) Å. A similar 2e$^-$ reduction of 1,2-diphenylhydrazine by (^{tbs}L)Fe$_3$(thf) affords (^{tbs}L)Fe$_3$(μ^3-NPh) and aniline. The solid state structure of (^{tbs}L)Fe$_3$(μ^3-NPh) is similar to the series of μ^3-nitrido and -imido triiron complexes synthesized in this work with average Fe−N$_{imido}$ and Fe−Fe bond lengths of 1.941(6) and 2.530(1) Å, respectively. Reductive N═N bond cleavage of azobenzene is also achieved in the presence of (^{tbs}L)Fe$_3$(thf) to yield triiron bis-imido complex (^{tbs}L)Fe$_3$(μ^3-NPh)(μ^2-NPh), which has been structurally characterized. Ligand redox participation has been ruled out, and therefore, charge balance indicates that the bis-imido cluster has undergone a 4e$^-$ metal based oxidation resulting in an (Fe^{IV})(Fe^{III})$_2$ formulation. Cyclic voltammograms of the series of triiron clusters presented herein demonstrate that oxidation states up to (Fe^{IV})(Fe^{III})$_2$ (in the case of [(^{tbs}L)Fe$_3$(μ^3-N)]NBu$_4$) are electrochemically accessible. These results highlight the efficacy of high-spin, polynuclear reaction sites to cooperatively mediate small molecule activation.

A. INTRODUCTION

Synthetic models of the polynuclear reaction centers found in both metalloenzyme cofactors and heterogeneous catalysts have been studied to reproduce the enhanced redox chemistry afforded by multiple metal centers.[1,2] However, the extent to which metal−metal interactions affect redox events and the role that polynuclear reaction sites play in substrate binding, breakdown, and functionalization are frequently not well understood.[3] For example, dinitrogen reduction occurs biologically by the nitrogenase enzymes[4−6] and abiologically by the high temperature, high pressure combination of hydrogen and nitrogen in the Haber Bosch process.[7] The precise sequence of chemical steps in either catalytic system remains elusive and has inspired a great deal of mechanistic study.[5,8,9] Biologically, the 6e^- reduction of dinitrogen to ammonia is achieved by the metalloenzyme nitrogenase[10] which contains FeMo, FeV, or Fe-only cofactors. Two hypotheses have been proposed regarding how N$_2$ activation occurs at the FeMoco of nitrogenase: (1) substrate uptake and reduction occurs at a single metal center, presumably Mo, by a Chatt-like mechanism;[11−13] or (2) a polynuclear iron face of the cluster mediates all requisite reaction chemistry.[14] The mononuclear hypothesis is predicated on the ability of molybdenum to access multiple oxidation states. Functional model complexes utilizing Mo have been shown to convert N$_2$ into ammonia and amine products.[15−18] However, site-mutagenesis at the valine residue α-70^{Val} located above the Fe2, Fe3, Fe6, Fe7 tetrairon face of FeMoco (Figure 1) inhibits substrate binding,[19,20] suggesting the polynuclear iron face could be the site of substrate uptake and activation.[1,21−23] While significant research efforts have focused on structural iron cluster models of the nitrogenase cofactor,[24−26] model complexes that test the viability of polynuclear reaction sites toward effecting multielectron reduction of small molecule substrates are less well studied.[28]

Received: May 20, 2013
Published: July 18, 2013

   dx.doi.org/10.1021/ja405057n | J. Am. Chem. Soc. 2013, 135, 12289−12296

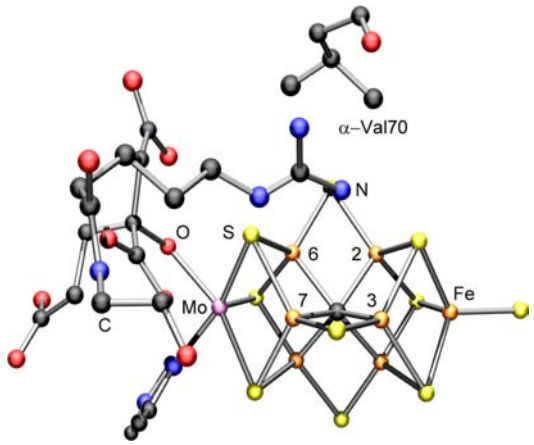

Figure 1. Nitrogenase FeMo-cofactor from Einsle et al.[27] (Mo pink, Fe orange, C black, N blue, O red, S yellow) where the α-70^{Val} residue and Fe(2367) tetrairon face are illustrated.

To test the ability of a polynuclear iron complex to mediate small molecule activation, we have designed flexible, multinucleating ligands to direct the formation of predesigned polynuclear architectures.[28−31] Using hexadentate ligand platforms comprising *o*-phenylenedianilide-based subunits, we have observed facile construction of polynuclear iron complexes whose intracore interactions (Fe−Fe: 2.274(1) −2.607(1) Å) and molecular spin states (S = 1 − 6) vary as a function of ligand architecture.[28,31] Within this family of iron cluster complexes, core-delocalized[28,30] as well as site-isolated redox events[33] with attendant ligand reorganization have been observed. Preparation of a triiron complex with the sterically restricted ligand variant, 1,3,5-C_6H_9(NHC$_6$H$_4$-*o*-NHSiMe$_2$^{t}Bu)$_3$(^{tbs}LH$_6$), afforded the complex (^{tbs}L)Fe$_3$(thf) (**1**) with a maximally high-spin ground state (S = 6).[28] Complex **1** is unique among coordination complexes of iron in that reaction with inorganic azide affords the trinuclear nitrido complex [(^{tbs}L)Fe$_3$(μ^3-N)]NBu$_4$ (**2a**) at ambient temperature without requiring photolysis of the azide (Scheme 1).[28] Here, we describe the two and four e^- reduction of hydrazine and diazene substrates, respectively, by the high-spin, all-ferrous complex **1** to afford imido and nitrido products.

B. EXPERIMENTAL SECTION

Materials and Methods. All manipulations involving metal complexes were carried out using standard Schlenk line or glovebox techniques under a dinitrogen atmosphere. All glassware was oven-dried for a minimum of 10 h and cooled in an evacuated antechamber prior to use in the drybox. Benzene, diethyl ether, hexanes and tetrahydrofuran (thf) were dried and deoxygenated on a Glass Contour System (SG Water USA, Nashua, NH) and stored over 4 Å molecular sieves (Strem) prior to use. Benzene-d_6 was purchased from Cambridge Isotope Laboratories and was degassed and stored over 4 Å molecular sieves prior to use. Nonhalogenated solvents were typically tested with a standard purple solution of sodium benzophenone ketyl in thf in order to confirm effective oxygen and moisture removal. Fe$_2$Mes$_4$ (Mes = 2,4,6-Me$_3$C$_6$H$_2$)[34] and TEMPOH (1-hydroxy-2,2,6,6-tetramethylpiperidine)[35] were prepared following published methods. All other reagents were purchased from commercial vendors and used without further purification unless explicitly stated.

Physical Measurements. All of the measurements for the metal complexes were made under anaerobic conditions. Elemental analyses were performed by Complete Analysis Laboratories, Inc., Parsippany, NJ. ^{1}H NMR spectra were recorded on Varian Unity/Inova 500B/600 NMR spectrometers with chemical shifts (δ ppm) referenced to residual NMR solvent. Solution magnetic susceptibilities were determined by Evans method using trifluoromethylbenzene as an internal reference. Gas chromatography−mass spectrometry (GC-MS) data was collected on a Shimadzu Gas-chromatograph (GCMS-QP2010S).

Zero-Field ^{57}Fe Mössbauer Spectroscopy. Zero-field, ^{57}Fe Mössbauer spectra were measured with a constant acceleration spectrometer (SEE Co, Minneapolis, MN). Solid or crystalline samples were prepared as Paratone-N mulls in a drybox and frozen in liquid nitrogen prior to handling in air. Isomer shifts are quoted relative to Fe metal at room temperature. Data was processed, fitted, and analyzed using an in-house package for IGOR Pro 6 (Wavemetrics, Lake Oswego, OR).

Synthesis. (^{tbs}L)Fe$_3$(thf) ***(1)***. The synthesis of (^{tbs}L)Fe$_3$(thf) has been previously reported.[28] If a small amount of (^{tbs}LH$_2$)Fe$_2$ is observed via ^{1}H NMR upon reacting ^{tbs}LH$_6$ with $^3/_2$ equivalents of Fe$_2$Mes$_4$, additional Fe$_2$Mes$_4$ was added until all of (^{tbs}LH$_2$)Fe$_2$ was consumed. [In the absence of coordinating solvent, formation of the diiron cluster (^{tbs}LH$_2$)Fe$_2$ is favored over formation of the triiron cluster. (^{tbs}LH$_2$)Fe$_2$ was synthesized from the reaction of Fe$_2$Mes$_4$ (41 mg, 0.070 mmol) and ^{tbs}LH$_6$ (50 mg, 0.067 mmol) in benzene at 75 °C for 18 h. ^{1}H NMR (benzene-d_6, 500 MHz, δ, ppm): 82.9, 52.3, 39.2, 37.7, 32.8, 25.0, 24.4, 23.2, 22.2, 20.1, 19.5, 14.5, 14.2, 12.9, 11.9, −2.31, −5.70, −15.2, −24.7, −32.2, −32.9, −34.0, −40.7. Full characterization of this compound will be provided in a future publication.] Lyophilization from benzene results in isolation of a black solid that can be stored −33 °C for several weeks. (^{tbs}L)Fe$_3$(thf) therefore does not need to be prepared immediately prior to subsequent reaction chemistry. Synthesis of (^{tbs}L)Fe$_3$(thf) can be run on a 0.500 g scale of ligand ^{tbs}LH$_6$.

*[(^{tbs}L)Fe$_3$(μ^3-N)]NBu$_4$ (**2a**)*. The synthesis of [(^{tbs}L)Fe$_3$(μ^3-N)]NBu$_4$ has been previously reported.[28] Upon reaction with purified (^{tbs}L)-Fe$_3$(thf) as described herein, it was determined that the previously reported ^{1}H NMR contained a small, unknown impurity that accounted for some of the minor peaks previously observed. If the impurity is present, it can be removed upon washing with cold diethyl ether, albeit a lower yield due to the solubility of **2a** in diethyl ether. If the impurity is not present, washing with cold hexanes results in a higher yield (95%). ^{1}H NMR (benzene-d_6, 500 MHz, δ, ppm): 55.9, 16.4, 7.50, 6.38, 3.87, 3.69, 1.96, 1.57, 0.70, −3.20.

*(^{tbs}L)Fe$_3$(μ^3-N)Li(thf)$_3$ (**2b**)*. Solid (^{tbs}L)Fe$_3$(μ^3-NH) (0.100 g, 0.108 mmol) (prepared as described below) was dissolved in 15 mL of cold thf (−33 °C). A cold solution of LiN(SiMe$_3$)$_2$ (0.018 g, 0.108 mmol) in 2 mL of thf was added dropwise to the solution of (^{tbs}L)Fe$_3$(μ^3-NH). The resulting mixture was allowed to stir at room temperature for 30 min. The volatiles were removed in vacuum, resulting in an oil. The oil was washed with hexanes (20 mL), and the resulting solid was dried. Isolated yield: 0.094 g (76%). ^{1}H NMR (benzene-d_6, 500 MHz, δ, ppm): 56.6, 16.7, 7.53, 6.70, 5.77, 4.88, 4.12, 3.85, 3.21, 1.24, −2.70. Anal. Calcd for C$_{54}$H$_{90}$Fe$_3$LiN$_7$O$_3$Si$_3$: C, 56.69; H, 7.93; N, 8.57. Found: C, 56.55; H, 7.88; N, 8.31. Zero-field ^{57}Fe Mössbauer (90 K) (δ, $|\Delta E_Q|$ (mm/s)): 0.33, *1.34*.

*(^{tbs}L)Fe$_3$(μ^3-NH) (**3**). Method 1.* Solid (^{tbs}L)Fe$_3$(thf) (0.069 g, 0.070 mmol) was dissolved in 15 mL of thf. A thf solution (2 mL) of phenylhydrazine (0.0076 g, 0.070 mmol) was added dropwise to the solution of (^{tbs}L)Fe$_3$(thf). (Note: It is important to run the reaction dilute to prevent formation of free ligand.) The reaction was then allowed to stir at room temperature for 1 h at which point the volatiles were removed in vacuum. In addition to (^{tbs}L)Fe$_3$(μ^3-NH), the crude product mixture contained aniline (1.6 mg, 0.017 mmol determined by ^{1}H NMR). [The formation of aniline was confirmed by ^{1}H NMR and GCMS. Aniline was isolated from the crude reaction mixture via flash column chromatography (solid support, silica; eluent, 10% methanol in dichloromethane) and was quantified by ^{1}H NMR using ferrocene as an internal standard. Due to solubility, the aniline could not be separated from the complex without the use of column chromatography. (^{tbs}L)Fe$_3$(μ^3-NH) does not survive the chromatographic process.] The resulting oil was lyophilized from benzene affording a solid. The product was dissolved in 5−10 mL of hexanes and filtered through a Celite plug. The hexanes were removed under reduced pressure, and the resulting product was lyophilized again from benzene to afford pure (^{tbs}L)Fe$_3$(μ^3-NH) in quantitative yield. Isolated yield: 61 mg (100%).

Method 2. Solid (^{tbs}L)Fe$_3$(thf) (0.065 g, 0.067 mmol) was dissolved in 15 mL of thf. A syringe was used to add 0.065 mL of a 1 M thf solution of hydrazine to 1 mL of thf. The resulting hydrazine solution was added dropwise to the solution of (^{tbs}L)Fe$_3$(thf). Upon stirring for 1 h at room temperature, the volatiles were removed in vacuum resulting in an oil. Lyophilization from benzene resulted in a brown solid. In the crude ^{1}H NMR, resonances that match that of (^{tbs}L)Fe$_3$(μ^3-NH) were identified (see Figure S1). Due to the solubility of the product and the impurities formed during the reaction, an isolated yield could not be obtained. A crude zero-field ^{57}Fe Mössbauer was obtained at 90 K [δ, $|\Delta E_Q|$ (mm/s) component 1 (28%) 0.37, *1.94* (Γ = 0.32 mm/s); component 2 (12%) 0.40, *1.17* (Γ = 0.18 mm/s); component 3 (60%) 0.55, *1.24* (Γ = 0.45 mm/s)] (Figure S11b). Vacuum transfer of the volatiles into a solution of 1 M HCl in diethylether resulted in trapping the NH_3 as the ammonium chloride salt (quantified by ^{1}H NMR using ferrocene as an internal standard, ranging from 14−70% isolated yield, Figure S2).

Method 3. Solid [(^{tbs}L)Fe$_3$(μ^3-N)]NBu$_4$ (0.040 g, 0.034 mmol) was dissolved in 9 mL of thf. A thf solution (1 mL) of lutidinium tetraphenylborate (0.015 g, 0.034 mmol) was added dropwise to the solution of [(^{tbs}L)Fe$_3$(μ^3-N)]NBu$_4$ at room temperature. The reaction was then allowed to stir at room temperature for 1 h at which point the volatiles were removed in vacuum. The resulting oil was lyophilized from benzene prior to the product being extracted into hexanes (10 mL). The hexane solution was dried and lyophilized from benzene, resulting in an oil. Isolated yield: 0.027 mg (85%).

*Spectroscopic Details for (^{tbs}L)Fe$_3$(μ^3-NH) (**3**).* ^{1}H NMR (benzene-d_6, 500 MHz, δ, ppm): 170, 56.3, 16.7, 8.36, 5.22, 3.38, 3.03, 2.86, 2.22, 1.94, −6.04. Anal. Calcd for $C_{42}H_{67}Fe_3N_7Si_3$: C, 54.72; H, 7.33; N 10.64. Found: C, 54.66; H, 7.41; N, 10.55. Zero-field ^{57}Fe Mössbauer (115 K) (δ, $|\Delta E_Q|$ (mm/s)): component 1: 0.37, *1.94* (78%); component 2: 0.40, *1.17* (22%).

*(^{tbs}L)Fe$_3$(μ^3-NPh) (**4**). Method 1.* Solid (^{tbs}L)Fe$_3$(thf) (0.060 g, 0.061 mmol) was dissolved in 15 mL of thf. A thf (1 mL) solution of 1,2-diphenylhydrazine (0.011 g, 0.061 mmol) was added dropwise to the solution of (^{tbs}L)Fe$_3$(thf) at room temperature (NOTE: It is important to run the reaction dilute to prevent formation of free ligand). The reaction was then allowed to stir at room temperature for 1 h at which point the volatiles were removed in vacuum, resulting in an oil. In addition to (^{tbs}L)Fe$_3$(μ^3-NPh), the crude product mixture contained aniline (3.3 mg, 0.035 mmol) and azobenzene (1.6 mg. 0.0086 mmol) determined by ^{1}H NMR. [The formation of aniline and azobenzene was confirmed by ^{1}H NMR and GCMS. Both the aniline and azobenzene were isolated by flash column chromatography (solid support: silica, eluent: 10% methanol in dichloromethane) and was quantified by ^{1}H NMR using ferrocene as an internal standard. Due to solubility, both the aniline and azobenzene could not be separated from the complex without the use of column chromatography. (^{tbs}L)Fe$_3$(μ^3-NPh) does not survive the chromatographic process. Aniline was also isolated upon column chromatography of (^{tbs}L)Fe$_3$(μ^3-NPh) synthesized by method 3.] The oil was lyophilized from benzene to afford a solid, which was then dissolved in 5−10 mL of hexanes and filtered through a Celite plug. The hexanes were removed under reduced pressure at which point the resulting oil was lyophilized again from benzene to afford clean (^{tbs}L)Fe$_3$(μ^3-NPh) as a solid. Isolated yield: 55 mg (83%).

Method 2. Solid (^{tbs}L)Fe$_3$(thf) (0.060 g, 0.061 mmol) was dissolved in 5 mL of benzene. A benzene solution of azobenzene (0.11 mL of a 50 mg/mL stock solution, 0.031 mmol) was added to the solution at room temperature. The reaction was subsequently heated to 80 °C for 4 days. The reaction also proceeds at room temperature, albeit with slower reaction times. In the crude ^{1}H NMR, resonances that match (^{tbs}L)Fe$_3$(μ^3-NPh) were identified (see Figure S3). Due to the solubility of the product and the impurities formed during the reaction, an isolated/crystalline yield could not be obtained. A crude zero-field ^{57}Fe Mössbauer was obtained at 90 K (δ, $|\Delta E_Q|$ (mm/s) component 1 (69%) 0.37, *1.72*; component 2 (31%) 0.41, *0.93* (Figure S13b).

Method 3. Solid (^{tbs}L)Fe$_3$(thf) (0.130 g, 0.134 mmol) was dissolved in 5 mL of cold thf (−33 °C). Phenylazide (0.0160 g, 0.134 mmol) in approximately 1 mL of thf was added to the solution of (^{tbs}L)Fe$_3$(thf). The reaction was allowed to stir at room temperature for 4 h at which point the volatiles were removed in vacuum. The resulting oil was lyophilized from benzene. Subsequently, the solid was dissolved in approximately 5 mL of cold (−33 °C) hexanes and filtered. The hexanes were removed in vacuum, and the resulting oil was lyophilized from benzene again, resulting in a brown solid. Isolated yield: 0.130 g (98%).

Method 4. Solid (^{tbs}L)Fe$_3$(thf) (0.014 g, 0.015 mmol) was dissolved in 0.5 mL of C_6D_6. A C_6D_6 solution (0.5 mL) of phenylhydrazine (0.0016 g, 0.015 mmol) was added dropwise to the solution of (^{tbs}L)Fe$_3$(thf) at room temperature in a J-Young tube. The reaction was allowed to sit at room temperature for 30 min, prior to heating at 80 °C for approximately 7 days. [The length of heating depended on the concentration and size of reaction vessel. Additional heating after full conversion to (^{tbs}L)Fe$_3$(μ^3-NPh) resulted in decomposition.] Vacuum transfer of the volatiles into a solution of 1 M HCl in diethylether resulted in trapping the NH_3 as the ammonium chloride salt (quantified by ^{1}H NMR using ferrocene as an internal standard, 7.9% isolated yield). The resulting solid was dissolved in hexanes and filtered through Celite. Removal of the solvent in vacuum resulted in isolation of (^{tbs}L)Fe$_3$(μ^3-NPh). Isolated yield: 7.8 mg (54%).

*Spectroscopic Details for (^{tbs}L)Fe$_3$(μ^3-NPh) (**4**).* ^{1}H NMR (benzene-d_6, 500 MHz, δ, ppm): 199.9, 62.2, 21.6, 9.17, 8.92, 4.26, 2.59, 2.47, −3.15, −3.85, −7.61, −13.3. Anal. Calcd for $C_{48}H_{71}Fe_3N_7Si_3$: C, 57.77; H, 7.17; N, 9.83. Found: C, 57.76; H, 6.98; N, 9.74. Zero-field ^{57}Fe Mössbauer (90 K) (δ, $|\Delta E_Q|$ (mm/s)): component 1: 0.42, *1.97* (67%); component 2: 0.42, *1.09* (33%).

*(^{tbs}L)Fe$_3$(μ^3-NPh)(μ^2-NPh) (**5**).* Solid (^{tbs}L)Fe$_3$(thf) (0.060 g, 0.061 mmol) was dissolved in 5 mL of C_6D_6. Azobenzene (0.011 g, 0.061 mmol) dissolved in 1 mL of C_6D_6 was added to the solution of (^{tbs}L)Fe$_3$(thf) and allowed to stir at room temperature for 24 h or at 80 °C for 1 h. The volatiles were removed in vacuum. X-ray quality crystals were grown from cold (−33 °C) heptane. Clean material for spectroscopic analysis was obtained by storing a concentrated hexanes or heptane solutions at −33 °C for several weeks, at which point polycrystalline material precipitated from solution. Crystalline yield: 0.011 g (17%). ^{1}H NMR (benzene-d_6, 500 MHz, δ, ppm): 45.1, 34.1, 27.9, 24.2, 22.1, 19.9, 17.2, 14.3, 9.16, 9.92, 6.73, 5.40, 2.47, 2.22, 2.16, 1.93, 0.18, −0.99, −1.21, −2.46, −3.56, −9.29, −13.0, −16.4, −20.1, −27.2, −38.0. Anal. Calcd for $C_{54}H_{76}Fe_3N_8Si_3$: C, 59.56; H, 7.03; N, 10.29. Found: C, 59.52; H, 6.96; N, 10.37. Zero-field ^{57}Fe Mössbauer (90 K) (δ, $|\Delta E_Q|$ (mm/s)): component 1: 0.24, *1.46* (21%); component 2: 0.45, *2.61* (18%); component 3: 0.34, *1.33* (60%).

*[(^{tbs}L)Fe$_3$(μ^3-Br)]NBu$_4$ (**6**).* Solid ^{tbs}LH$_6$ (0.100 g, 0.134 mmol) was dissolved in 10 mL of thf. The solution was added to solid Fe$_2$Mes$_4$ (0.123 g, 0.208 mmol) at room temperature. The reaction was heated in a sealed bomb at 75 °C for 12 h. Solid Br[NBu$_4$] (0.048 g, 0.149 mmol) was added to the reaction mixture cold (−33 °C). Once the reaction reached room temperature, the solution was stirred for an additional 4 h. The volatiles were removed in vacuum resulting in a brown oil. The brown oil was stirred in diethyl ether (10 mL) for 15 min and precipitated and collected on a pad of Celite. The precipitate was dissolved in thf (2 mL), dried in vacuum, and lyophilized from benzene to afford a solid. Isolated yield: 141 mg, (85%). X-ray quality crystals were grown from diethyl ether at −33 °C. ^{1}H NMR (benzene-d_6, 500 MHz, δ, ppm): 198, 44.4, 37.4, 6.31, 3.54, 1.91, 1.37, 0.92, 0.15, −40.2. Anal. Calcd for $C_{58}H_{102}Fe_3BrN_7Si_3$: C, 56.67; H, 8.36; N, 7.98. Found: C, 56.63; H, 8.35; N, 7.88. Zero-field ^{57}Fe Mössbauer (110 K) (δ, $|\Delta E_Q|$ (mm/s)): 0.71, *1.35*.

Reaction of (^{tbs}L)Fe$_3$(μ^3-NH) with TEMPOH. A thf (0.5 mL) solution of TEMPOH (1-hydroxy-2,2,6,6-tetramethylpiperidine) (0.013 g, 0.083 mmol) is added to a frozen thf solution of (^{tbs}L)Fe$_3$(μ^3-NH) (0.025 g, 0.027 mmol) and Bu$_4$NBr (0.0097 g, 0.030 mmol) in a J-Young NMR tube. The mixture is allowed to thaw and sit at room temperature for 3 h at which point all of the paramagnetic features in the ^{1}H NMR associated with **3** are no longer present. Vacuum transfer of the volatiles into a solution of 1 M HCl in diethylether resulted in trapping the NH_3 as the ammonium chloride salt (quantified by ^{1}H NMR using ferrocene as an internal standard, 13% isolated yield).

Table 1. Structural, Spectral, and Magnetic Properties of Select Complexes

complex		Fe−Fe$_{avg}$ (Å)	μ_{eff} (μ_B)	δ (mm/s) (% component)	$\lvert\Delta E_Q\rvert$ (mm/s)	ref
(^{tbs}L)Fe$_3$(thf)	**1**	2.577(6)	12.0(2)	0.89 (24)	1.68	28
				0.49 (35)	1.55	
				0.50 (41)	1.92	
[(^{tbs}L)Fe$_3$(μ^3-N)][NBu$_4$]	**2a**	2.480(1)	7.3(2)	0.37 (30)	1.78	28
				0.39 (70)	1.23	
[(^{tbs}L)Fe$_3$(μ^3-N)]Li(thf)$_3$	**2b**	2.480(1)		0.33	1.34	
(^{tbs}L)Fe$_3$(μ^3-NH)	**3**		5.8(1)	0.37 (78)	1.94	
				0.40 (22)	1.17	
(^{tbs}L)Fe$_3$(μ^3-NPh)	**4**	2.530(1)	6.6(4)	0.42 (67)	1.97	
				0.42 (33)	1.09	
(^{tbs}L)Fe$_3$(μ^3-NPh)(μ^2-NPh)	**5**	2.684(1)		0.24 (21)	1.46	
				0.45 (18)	2.61	
				0.34 (60)	1.33	
(^{tbs}L)Fe$_3$(μ^3-NMe)		2.483(3)	5.3(2)	0.37 (28)	0.94	28
				0.36 (72)	1.67	
Fe$_4$(μ^3-N^{t}Bu)$_4$Cl$_4$				0.35	0.55	36
[Fe$_4$(μ^3-N^{t}Bu)$_4$(N^{t}Bu)Cl$_3$]				−0.17 (21)	0.38	36
				0.36 (79)	0.43	
[(^{tbs}L)Fe$_3$(μ^3-Br)]NBu$_4$	**6**	2.771(9)	11.9(4)	0.71	1.35	
(^{H}L)Fe$_3$(PMe$_3$)$_3$		2.300(2)	3.0	0.38	1.03	30

C. RESULTS AND DISCUSSION

Treatment of triiron cluster **1** with phenylhydrazine (Scheme 1) at room temperature results in the quantitative formation of the triiron imido complex (^{tbs}L)Fe$_3$(μ^3-NH) (**3**) and aniline (24% isolated yield, identified and quantified by ^{1}H NMR spectroscopy) with no detectable formation of ammonia during the course of the reaction. Complex **3** exhibits a paramagnetically shifted ^{1}H NMR spectrum featuring eleven proton resonances, suggestive of a C_3-symmetric species in solution. The solution magnetic moment of complex **3** was 5.8(1) μ_B (C_6D_6, 298 K) as determined by the Evans method. The zero-field ^{57}Fe Mössbauer spectrum, featuring two quadrupole doublets (δ, $\lvert\Delta E_Q\rvert$ (mm/s): component 1: 0.37, *1.94* (78%); component 2: 0.40, *1.17* (22%)), is similar to that observed for nitrido anion **2a** (see Table 1 for comparison of spectroscopic features) and is consistent with a delocalized 2e^- oxidation at the triiron core. The two quadrupole doublets observed in the Mössbauer spectrum of **2a** and **3** arise from deviation of the complex from rigorous C_3-symmetry in the solid-state (see bond metrics Figure 1). The solution IR spectrum of **3** shows a weak vibration at 3363 cm^{-1}, consistent with an N−H stretch. Substituting hydrazine for phenylhydrazine in the reaction with **1** produces **3** as determined by ^{1}H NMR (Figure S1) with liberation of ammonia as detected by ^{1}H NMR (following vacuum transfer of the reaction volatiles into a HCl/Et$_2$O solution, Figure S2). However, the reaction with hydrazine is not as clean, as **3** is not exclusively formed during this reaction as evident by ^{1}H NMR and ^{57}Fe Mössbauer of the crude reaction mixture.

Despite the high yield of the paramagnetic product **3** during the reaction of **1** with phenylhydrazine, the high solubility of **3** made obtaining crystals suitable for X-ray crystallographic analysis difficult. To support our assignment of **3** as the triiron parent μ^3-imido cluster, we sought to synthesize the μ^3-imido species via an alternative route. Addition of lutidinium tetraphenylborate to [(^{tbs}L)Fe$_3$(μ^3-N)]NBu$_4$ (**2a**) results in formation of a neutral product in 85% isolated yield featuring an identical paramagnetic ^{1}H NMR spectrum to that assigned as **3** (Figure S1, Scheme 1). Additionally, ammonia can be evolved from complex **3** via addition of a suitable H-atom transfer reagent such as TEMPO-H (1-hydroxy-2,2,6,6-tetramethylpiperidine), as identified by ^{1}H NMR spectroscopy following vacuum transfer of the reaction volatiles.

Deprotonation of **3** with lithium bis(trimethylsilyl)amide results in formation of the triiron nitrido complex capped with a thf-solvated Li cation [(^{tbs}L)Fe$_3$(μ^3-N)]Li(thf)$_3$ (**2b**) in 76% isolated yield (Scheme 1). Single crystals of **2b** suitable for crystallographic analysis were obtained from a diethylether solution at −33 °C. The crystallographically determined bond metrics for lithium-capped **2b** are similar to the naked nitride product previously reported[28] but features a rigorously C_3-symmetric complex (space group $Pa\bar{3}$) Fe−Fe 2.4802(5), Fe−N3 1.877(2), N3−Li 1.990(6) (Figure 2a). The rigorous C_3-symmetry observed in the solid-state also manifests spectroscopically as a single quadrupole doublet being observed in the Mössbauer spectrum (δ, $\lvert\Delta E_Q\rvert$ (mm/s): 0.33, *1.34*) (Figure 3a).

While the kinetic product in the reaction of phenylhydrazine with **1** is the parent imido complex **3**, heating the crude reaction mixture (**3** and aniline) at 80 °C for 7 days produced a new, paramagnetic product distinct from **3** with concomitant formation of ammonia (identified via ^{1}H NMR following vacuum transfer of the reaction volatiles). The similarities between the ^{1}H NMR spectra of this new species with **3** suggests a transamination has occurred between (^{tbs}L)Fe$_3$(μ^3-NH) and aniline remaining from phenylhydrazine reduction to yield the phenylimido product (^{tbs}L)Fe$_3$(μ^3-NPh) (**4**) (Scheme 1). Addition of a thf solution of 1,2-diphenylhydrazine to **1** in thf also produces **4** (determined by ^{1}H NMR spectroscopy) in 83% isolated yield and free aniline (identified and quantified by ^{1}H NMR). Complex **4** could also be synthesized by treatment of triiron cluster **1** with phenyl azide in a 98% yield (Scheme 1). Zero-field ^{57}Fe Mössbauer analysis **4** features two quadrupole doublets [δ, $\lvert\Delta E_Q\rvert$ (mm/s): component 1: 0.42, *1.97* (67%); component 2: 0.42, *1.09* (33%)] (Figure 3b), with similar parameters to **2** and **3**. Single crystals from the reaction of **1** with phenyl azide were grown from cold hexanes and contained the μ^3-phenylimido species (^{tbs}L)Fe$_3$(μ^3-NPh) (**4**) (6.6(4) μ_B; Figure 2b). Complex **4** is structurally similar to the previously reported methyl imido complex (^{tbs}L)Fe$_3$(μ^3-NMe),[28] featuring

Scheme 1

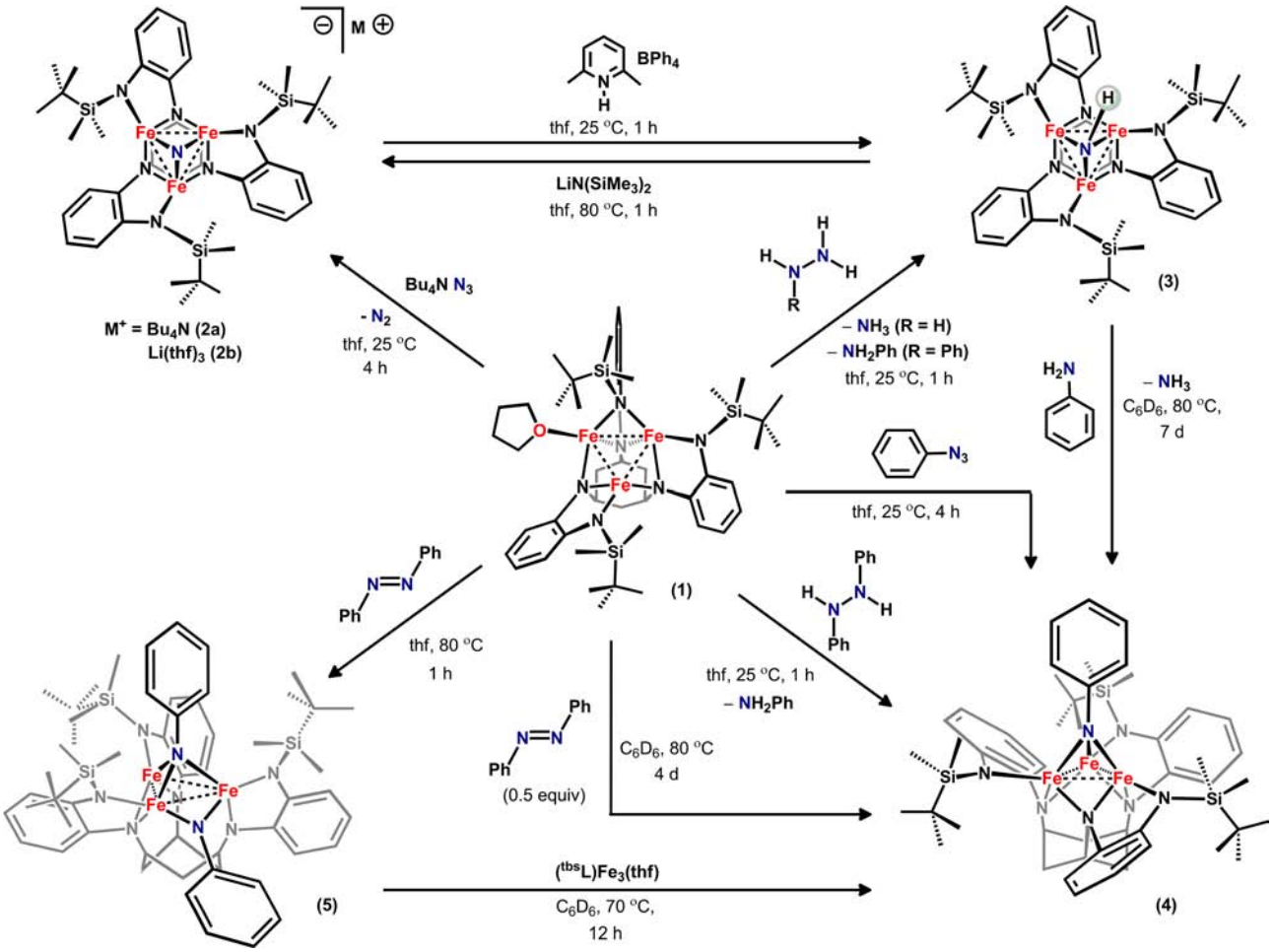

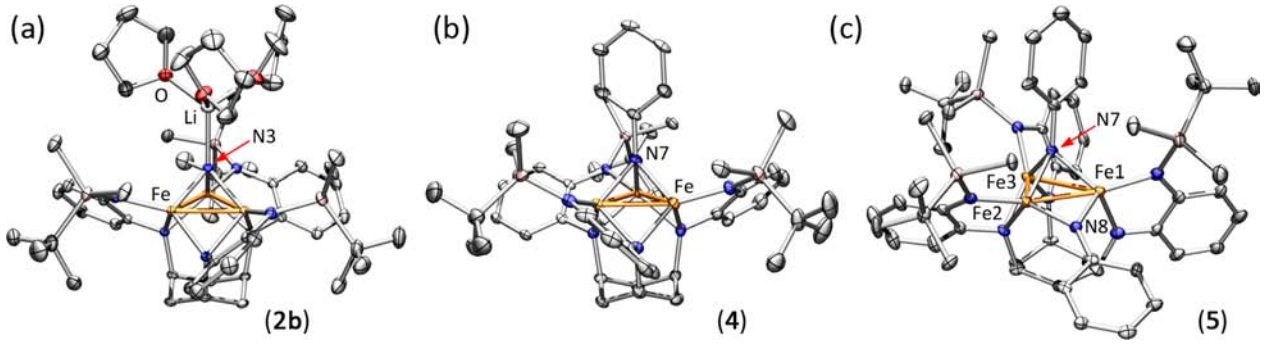

Figure 2. Solid-state structures for (a) [(^{tbs}L)Fe$_3$(μ^3-N)]Li(thf)$_3$ (**2b**), (^{tbs}L)Fe$_3$(μ^3-NPh) (**4**), and (^{tbs}L)Fe$_3$(μ^3-NPh)(μ^2-NPh) (**5**) with the thermal ellipsoids set at the 50% probability level (hydrogen atoms and solvent molecules omitted for clarity; Fe orange, C gray, N blue, O red, Si pink, Li white). Selected bond lengths (Å) for (**2b**): Fe–Fe 2.4802(5), Fe–N3 1.877(2), N3–Li 1.990(6); for (**4**): Fe1–Fe2 2.549(1), Fe1–Fe3 2.502(1), Fe2–Fe3 2.539(1), Fe1–N7 1.935(5), Fe2–N7 1.944(5), Fe3–N7 1.944(5); for (**5**): Fe1–Fe2 2.482(1), Fe1–Fe3 2.966(1), Fe2–Fe3 2.604(1), Fe1–N7 1.973(4), Fe2–N7 1.982(4), Fe3–N7 1.904(4), Fe1–N8 1.866(4), Fe2–N8 1.848(4).

a central μ^3-imido ligand with average Fe–N$_{imido}$ and Fe–Fe bond lengths of 1.941(6) Å and 2.530(1) Å, respectively (Table 1).

With the knowledge that complex **1** could readily activate the N–N bonds in hydrazine and inorganic and organic azides, we investigated the reaction of **1** and azobenzene. Addition of 0.5–1 equiv of azobenzene to compound **1** at 80 °C for 4 days leads to the formation of phenylimido **4** as the major paramagnetic product as identified by ^{1}H NMR (Figure S3) and Mössbauer spectroscopies (Figure S13b) (Scheme 1). This reaction is also observed to proceed at room temperature, albeit over longer reaction times. Monitoring the reaction progression by ^{1}H NMR, we find that complex **4** is not the first observable species detected upon addition of azobenzene to **1**. The initial product formed exhibits paramagnetically-shifted ^{1}H resonances that diminish over time to yield the thermodynamic product **4**. Addition of one equivalent of azobenzene to **1** followed by heating at 80 °C for one hour generated this intermediate prior to the appearance of compound **4** as ascertained by ^{1}H NMR. Storage of this product at −33 °C in a mixture of hexane and heptane precipitated a quantity of polycrystalline material suitable for isolation and

dx.doi.org/10.1021/ja405057n | J. Am. Chem. Soc. 2013, 135, 12289–12296

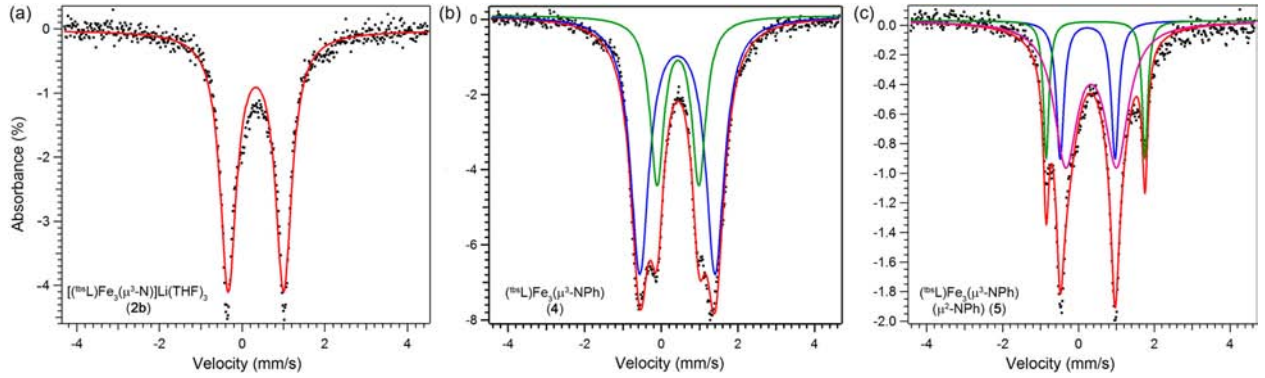

Figure 3. Zero-field ^{57}Fe Mössbauer spectrum of (a) [(^{tbs}L)Fe$_3$(μ^3-N)]Li(thf)$_3$ (**2b**), (b) (^{tbs}L)Fe$_3$(μ^3-NPh) (**4**), and (c) (^{tbs}L)Fe$_3$(μ^3-NPh)(μ^2-NPh) (**5**) obtained at 90 K. Simulation yields the following parameters [δ, $|\Delta E_Q|$ (mm/s)] for **2b**: 0.33, *1.34* (Γ = 0.24 mm/s); for **4**: component 1 (blue, 67%) 0.42, *1.97* (Γ = 0.29 mm/s); component 2 (green, 33%) 0.42, *1.09* (Γ = 0.22 mm/s); and for **5**: component 1 (blue, 21%) 0.24, *1.46* (Γ = 0.12 mm/s); component 2 (green, 18%) 0.45, *2.61* (Γ = 0.10 mm/s); component 3 (magenta, 60%) 0.34, *1.33* (Γ = 0.36 mm/s).

analysis (17% crystalline yield). Treatment of this intermediate with 1 equivalent of **1** (70 °C, 12h) produces the phenylimido product **4** (as identified by ^{1}H NMR, Figure S5), suggesting that the intermediate is either a triiron azobenzene adduct or a triiron complex containing two imido functionalities following azobenzene activation. Crystallization from a concentrated heptane solution at −33 °C produced crystals suitable for X-ray diffraction analysis. The solid-state structure revealed the intermediate as the triiron bis-imido cluster (^{tbs}L)Fe$_3$(μ^3-NPh)(μ^2-NPh) (**5**) in which **1** has been oxidized by 4e^- and the N═N double bond of azobenzene has been cleaved (Scheme 1, Figure 2c). The crystal structure of complex **5** features two molecules in the asymmetric unit with several structural features similar to **4**, most notably a central μ^3-imido ligand. While the average μ^3−imido−iron bond lengths in **4** and **5** are nearly identical (1.941(6) and 1.953(5) Å, respectively), the Fe−Fe separations in **5** are significantly elongated from **4** (molecule A: Fe1−Fe2 2.482(1) Å; Fe1−Fe3 2.966(1) Å; Fe2−Fe3 2.604(1) Å; molecule B: Fe4−Fe5 2.481(1) Å; Fe4−Fe6 3.244(1) Å; Fe5−Fe6 2.594(1) Å) (Table 1). The average Fe−N distance to the μ^2-imido ligand is shorter than that to the μ^3-imido ligand (1.857(5) and 1.953(5) Å respectively). In order to accommodate the second imido unit bound to iron centers Fe1 and Fe2 (Figure 2c), the (^{tbs}L)$^{6-}$ ligand anilido groups have reorganized to optimize the bonding interaction with the two imido moieties. Such ligand reorganization has been previously reported upon oxidation of high-spin iron clusters.[33] Each of the (^{tbs}L)$^{6-}$ ligand peripheral anilido groups remain terminally bound to a single iron center, only one of the three internal alkyl aryl anilido moieties (N2) bridge adjacent metal centers.

Charge balance would indicate that bis-imido cluster **5** has undergone a four-electron oxidation, suggesting an (Fe^{IV})(Fe^{III})$_2$ formulation. Ligand redox participation in the observed oxidation event was ruled out by comparing the N−C and C−C bond metrics in the *o*-phenylenedianilido subunits of the (^{tbs}L)$^{6-}$ ligand in **5** to that of the starting material **1** and oxidized complexes **2**−**4** (Table S5 in the Supporting Information). Comparison of the iron-ligand anilido bond distances within cluster **5** does not reveal which metal center bears the 4+ charge (Table S4). The zero-field ^{57}Fe Mössbauer spectrum of bis-imido complex **5** (Figure 3c) was fit with three quadrupole doublets (δ, $|\Delta E_Q|$ (mm/s): component 1: 0.24, *1.46* (21%); component 2: 0.45, *2.61* (18%); component 3: 0.34, *1.35* (60%); Table 1). The isomer shifts observed for **5** are lower relative to those observed in the 2e^- oxidized clusters in **2**−**4**, though a rigorous comparison between species cannot be made given the dramatic changes observed for the local iron coordination environments. Lee and co-workers have reported iron-imido cubane complexes and observed isomer shifts at ∼0.35 mm/s for high-spin iron(III) clusters Fe$_4$(μ^3-N^{t}Bu)$_4$Cl$_4$ and [Fe$_4$(μ^3-N^{t}Bu)$_4$(N^{t}Bu)Cl$_3$], while [Fe$_4$(μ^3-N^{t}Bu)$_4$(N^{t}Bu)Cl$_3$] exhibits an isomer shift of −0.17 mm/s for the Fe^{IV} center bound to a terminal imido group (Table 1).[36] We hypothesize that the overall higher isomer shifts of 0.24, 0.34, and 0.45 mm/s for compound **5** relative to Lee's iron imido cubanes could be due to cooperative binding of the imido moieties to multiple metal centers. Imido ligand binding to multiple metal centers may result in an overall decrease in e^- donation thereby deshielding the 1*s* orbital less at each metal center relative to that if the substrate was bound to a single metal center.

The presence of a formally tetra-valent iron center in **5** prompted us to investigate the redox limits of the complexes presented herein. Cyclic voltammograms of clusters **2a**, **3**, **4**, and isostructural, all-ferrous triiron cluster [(^{tbs}L)Fe$_3$(μ^3-Br)]NBu$_4$ (**6**) were collected (Figure 4, Table 2). The cyclic voltammograms

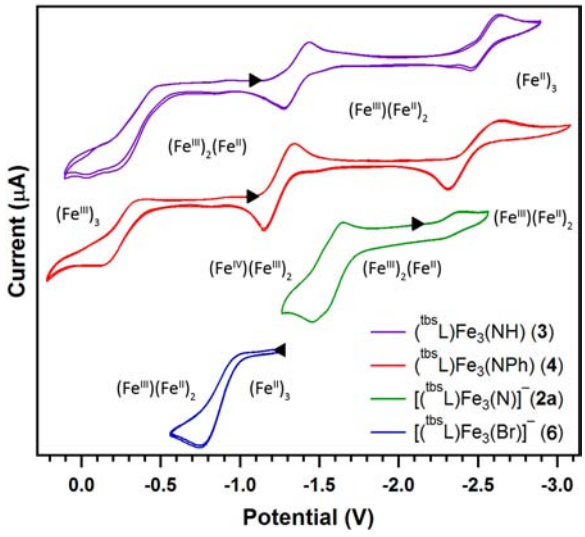

Figure 4. Cyclic voltammograms for (purple) (^{tbs}L)Fe$_3$(μ^3-NH) (**3**), (red) (^{tbs}L)Fe$_3$(μ^3-NPh) (**4**), (green) [(^{tbs}L)Fe$_3$(μ^3-N)]$^-$ (**2a**), and (purple) [(^{tbs}L)Fe$_3$(μ^3-Br)]$^-$ (**6**) (2-3 mM analyte, 0.1 M [Bu$_4$N]PF$_6$, glassy C working electrode, scan rate 0.01 V/s in thf, referenced to [Cp$_2$Fe]$^{+/0}$).

dx.doi.org/10.1021/ja405057n | J. Am. Chem. Soc. 2013, 135, 12289−12296

Table 2. Redox Potentials of Select Compounds

	open circuit potential (V)[a]	redox potential (V)[a]	oxidation event
2a	−2.25	−1.48	$(Fe^{III})_3 \rightarrow (Fe^{IV})(Fe^{III})_2$
		−1.60	$(Fe^{III})_2(Fe^{II}) \rightarrow (Fe^{III})_3$
		−2.41[c]	$(Fe^{III})(Fe^{II})_2 \rightarrow (Fe^{III})_2(Fe^{II})$
3	−1.14	−0.20[b]	$(Fe^{III})_2(Fe^{II}) \rightarrow (Fe^{III})_3$
		−1.36	$(Fe^{III})(Fe^{II})_2 \rightarrow (Fe^{III})_2(Fe^{II})$
		−2.54	$(Fe^{II})_3 \rightarrow (Fe^{III})(Fe^{II})_2$
4	−1.13	−0.12[b]	$(Fe^{III})_2(Fe^{II}) \rightarrow (Fe^{III})_3$
		−1.25	$(Fe^{III})(Fe^{II})_2 \rightarrow (Fe^{III})_2(Fe^{II})$
		−2.48	$(Fe^{II})_3 \rightarrow (Fe^{III})(Fe^{II})_2$
6	−1.29	−0.74[b]	$(Fe^{II})_3 \rightarrow (Fe^{III})(Fe^{II})_2$

[a]Referenced to $[Cp_2Fe]^{+/0}$; [b]Peak anodic current; [c]Peak cathodic current.

for both imido triiron clusters **3** and **4** feature three well-separated redox events and possess nearly identical open circuit potentials (−1.14 and −1.13 V, respectively). Each imido complex exhibits two quasi-reversible one-electron reduction processes [$E_{1/2}$ (V) for **3**: −1.36, −2.54; for **4**: −1.25, −2.48] as well as a single irreversible one-electron oxidation event [peak anodic current (V) for **3**: −0.20; for **4**: −0.12]. These electrochemical events suggest that the imido complexes can traverse three molecular redox states, which we formulate as $(Fe^{II})_3 \rightarrow (Fe^{III})_3$, as annotated in Figure 4. Examination of the nitrido complex **2a**, we observe a substantial shift in the open circuit potential (−2.25 V) and two nearly coincident quasi-reversible one-electron oxidation events at lower potentials [$E_{1/2}$ (V): −1.48, −1.60]; indicating the nitrido **2a** can be doubly oxidized, suggesting a $(Fe^{III})_2(Fe^{II}) \rightarrow (Fe^{IV})(Fe^{III})_2$ redox change. Thus, accessing a tetravalent state is not limited to complexes bearing multiple functionalities to the trinuclear core as in **5**.

Comparing the first oxidation $[(Fe^{II})_3 \rightarrow (Fe^{III})(Fe^{II})_2]$ for the series of complexes of the type $(^{tbs}L)Fe_3(\mu^3\text{-}E)$ (where E = N in **2a**, NH in **3**, NPh in **4**, Br in **6**) reveals a considerable shift in redox potentials. For imido complexes **3** and **4**, this redox event occurs near −2.5 V, whereas for the Br adduct **6** this redox couple is observed at −0.74 V. For the nitride **2a**, this redox couple is not observed, but the $[(Fe^{III})(Fe^{II})_2 \rightarrow (Fe^{III})_2(Fe^{II})]$ redox event occurs at −2.35 V. A substantial cathodic shifting is observed upon exchange of the μ^3-ligand from the Br adduct (**6**), to imido ligands (**3**, **4**), to the nitrido ligand (**2a**). This cathodic shift on going from Br anion (**6**) to the neutral imidos (**3**, **4**) results from the enhanced Fe−Fe interactions found in the imidos (average Fe−Fe: 2.530(1) Å in **4**) that is not present in the Br anion (average Fe−Fe: 2.769(1) Å in **6**). Although the nitride **2a** is isoelectronic with the imidos, the Fe−Fe separation shortens further (average Fe−Fe: 2.483(1) Å in **2a**) and the negative charge for the complex cathodically shifts the redox potentials even further as observed. The charge of the complex, close Fe−Fe interactions, and the hexa-anionic ($^{tbs}L^{6-}$) ligand platform all contribute to the highly cathodically-shifted materials reported herein.

D. CONCLUSIONS

The results herein highlight the advantages that polynuclear reaction sites can offer as a design strategy for small molecule activation. (1) The polynuclear reaction site allows small molecule binding and activation. Upon exposure of the triiron cluster $(^{tbs}L)Fe_3(thf)$ to hydrazine or phenylhydrazine, normally employed as reducing agents, the core is oxidized to yield triiron μ^3-imido complexes with liberation of ammonia (or aniline). Furthermore, complex **1** also facilitates the $4e^-$ reduction of azobenzene to yield triiron bis-imido cluster $(^{tbs}L)Fe_3(\mu^3\text{-}NPh)(\mu^2\text{-}NPh)$. While iron compounds have been shown to reduce hydrazines,[37−43] there are fewer examples in which iron facilitates the N=N bond cleavage.[44,45] For example, low-valent trinuclear Fe(0) carbonyl clusters facilitates thermolytic N=N bond cleavage of azoalkanes.[44] Our system demonstrates that low oxidation state clusters are not required to achieve multielectron reduction of substrate. The hexa-anionic $(^{tbs}L)^{6-}$ provides a very reducing environment for the trinuclear core as well as permitting Fe−Fe interactions to occur within the core. Both of these factors contribute to the substantial cathodic shifting observed for the trinuclear species, as well as the potent reduction chemistry observed, highlighted by the four-electron reduction of azobenzene at room temperature. (2) The open-shell electronic configuration of the all-ferrous starting material allows for facile ligand reorganization which promotes desirable reactivity. As substrate is engaged, ligand rearrangement occurs without inducing a large energetic penalty. The resulting products maintain a high-spin configuration, which renders the imido and nitrido moieties reactive toward further modification. For example, the triiron bis-imido cluster $(^{tbs}L)Fe_3(\mu^3\text{-}NPh)(\mu^2\text{-}NPh)$ is capable of transferring an imido unit to another triiron cluster. Additionally, the reactive triiron cluster $(^{tbs}L)Fe_3(\mu^3\text{-}NH)$ can liberate ammonia upon exposure to the $H^\bullet$ source TEMPO-H or via transamination with aniline to generate $(^{tbs}L)Fe_3(\mu^3\text{-}NPh)$. (3) The close M−M interactions facilitate redox distribution within the core and significantly contribute to the cathodic shifting observed for the complexes reported herein. Along with the close Fe−Fe bonding interactions, the hexa-anionic $(^{tbs}L)^{6-}$ platform and the charge of the molecule all contribute to the electron-richness of the imido and nitrido species. This cumulative effect is highlighted as the nitride complex reported is the most reducing species in the series examined. This observation should be contrasted to terminal iron nitride complexes wherein the nitrides are typically not amenable to further oxidation.[46−49]

Through our investigation, we have demonstrated that in the absence of a protein superstructure, a high-spin, all-ferrous polynuclear cluster is capable of undergoing cooperative multielectron reduction of small molecule substrates. The iron cluster presented herein stabilizes potential chemical species along the dinitrogen activation pathway, including imido and nitrido moieties. Even upon oxidation, the clusters maintain open-shell configurations and are highly reducing as a result of electron-rich ligand environments and close Fe−Fe interactions. The redox flexibility inherent to the polynuclear complexes make them compelling platforms on which small molecule activation processes can be pursued. Small molecule catalysts capable of concerted delivery of multiple reducing or oxidizing equivalents to substrate could circumvent the large overpotential penalty incurred traversing single electron pathways.[50] By demonstrating the ability of polynuclear reaction sites to effect multielectron reduction of substrates, we have taken important strides toward this goal and begun to collect evidence in support of the polynuclear hypothesis.

■ ASSOCIATED CONTENT

Supporting Information

Spectral data for **2b**, **3**, **4**, **5**, and **6**; selected crystallographic data and bond lengths for **2b**, **3**, **4**, **5**, and **6**; CIF file for **2b**, **3**, **4**, **5**, and

6. This material is available free of charge via the Internet at http://pubs.acs.org.

AUTHOR INFORMATION

Corresponding Author

betley@chemistry.harvard.edu

Notes

The authors declare no competing financial interest.

ACKNOWLEDGMENTS

This work was supported by a grant from the NIH (GM 098395) and Harvard University. T.M.P. is grateful for support from the Novartis Graduate Fellowship in Chemical Sciences for Minorities and Women and the Marie Hong fellowship. T.A.B. is grateful for a George W. Merck Fellowship. We thank S.-L. Zheng (Harvard) for help with X-ray crystallographic analysis and E. Hennessy for assistance with mass spectrometry. The crystallographic data CCDC 895634 and 923225−923227 can be obtained free at www.ccdc.cam.ac.uk/data_request/cif (or from Cambridge Crystallographic Data Centre, 12 Union Road, Cambridge, CB2 1EZ, UK; fax: ++44-1223-336-033; email: deposit@ccdc.cam.ac.uk).

REFERENCES

(1) Seefeldt, L. C.; Dance, I. G.; Dean, D. R. *Biochemistry* **2004**, *43*, 1401.
(2) Muetterties, E. L. *Science* **1977**, *196*, 839.
(3) Holm, R. H.; Kennepohl, P.; Solomon, E. I. *Chem. Rev.* **1996**, *96*, 2239.
(4) Eady, R. R. *Coord. Chem. Rev.* **2003**, *237*, 23.
(5) Burgess, B. K.; Lowe, D. J. *Chem. Rev.* **1996**, *96*, 2983.
(6) Howard, J. B.; Rees, D. C. *Chem. Rev.* **1996**, *96*, 2965.
(7) Travis, T. *Chem. Ind.* **1993**, 581.
(8) Bozso, F.; Ertl, G.; Grunze, M.; Weiss, M. *J. Catal.* **1977**, *49*, 18.
(9) Ertl, G. *J. Vac. Sci. Technol.* **1983**, *1*, 1247.
(10) Simpson, F. B.; Burris, R. H. *Science* **1984**, *224*, 1095.
(11) Pickett, C. J. *J. Biol. Inorg. Chem.* **1996**, *1*, 601.
(12) Peters, J. C.; Mehn, M. P. Bio-organometallic Approaches to Nitrogen Fixation Chemistry. In *Activation of Small Molecules*; Tolman, W. B., Ed.; Wiley: Weinheim, Germany, 2006; pp 81−119.
(13) Holland, P. L. Nitrogen Fixation. In *Comprehensive Coordination Chemistry II*; McCleverty, J. A., Meyer, T. J.; Eds.; Elsevier: Oxford, 2004; Vol. *8*, pp 569−599.
(14) Seefeldt, L. C.; Dance, I. G.; Dean, D. R. *Biochemistry* **2004**, *43*, 1401.
(15) Pickett, C. J.; Talarmin, J. *Nature* **1985**, *317*, 652.
(16) Yandulov, D. V.; Schrock, R. R. *Science* **2003**, *301*, 76.
(17) Shilov, A. E. *Russ. Chem. Bull. Int. Ed.* **2003**, *52*, 2555.
(18) Arashiba, K.; Miyake, Y.; Nishibayashi, Y. *Nature Chem.* **2011**, *3*, 120.
(19) Barney, B. M.; Igarashi, R. Y.; Dos Santos, P. C.; Dean, D. R.; Seefeldt, L. C. *J. Biol. Chem.* **2004**, *279*, 53621.
(20) Dos Santos, P. C.; Igarashi, R. Y.; Lee, H.-I.; hoffman, B. M.; Seefeldt, L. C.; Dean, D. R. *Acc. Chem. Res.* **2005**, *38*, 208.
(21) Christiansen, J.; Cash, V. L.; Seefeldt, L. C.; Dean, D. R. *J. Biol. Chem.* **2000**, *275*, 11459.
(22) Mayer, S. M; Niehaus, W. G.; Dean, D. R. *J. Chem. Soc., Dalton Trans.* **2002**, 802.
(23) Lee, H.-I.; Igarashi, R.; Laryukhin, M.; Doan, P. E.; Dos Santos, P. C.; Dean, D. R.; Seefeldt, L. C.; Hoffman, B. M. *J. Am. Chem. Soc.* **2004**, *126*, 9563.
(24) Lee, S. C.; Holm, R. H. *Chem. Rev.* **2004**, *104*, 1135.
(25) Han, J.; Beck, K.; Ockwig, N.; Coucouvanis, D. *J. Am. Chem. Soc.* **1999**, *121*, 10448.
(26) Coucouvanis, D.; Han, J.; Moon, N. *J. Am. Chem. Soc.* **2002**, *124*, 216.
(27) Einsle, O.; Tezcan, F. A.; Andrade, S. L. A.; Schmid, B.; Yoshida, M.; Howard, J. B.; Rees, D. C. *Science* **2002**, *297*, 1696.
(28) Powers, T. M.; Fout, A. R.; Zheng, S.-L.; Betley, T. A. *J. Am. Chem. Soc.* **2011**, *133*, 3336.
(29) Fout, A. R.; Xiao, D. J.; Zhao, Q.; Harris, T. D.; King, E. R.; Eames, E. V.; Zheng, S.; Betley, T. A. *Inorg. Chem.* **2012**, *19*, 10290.
(30) Zhao, Q.; Betley, T. A. *Angew. Chem., Int. Ed.* **2011**, *50*, 709.
(31) Eames, E. V.; Harris, T. D.; Betley, T. A. *Chem. Sci.* **2012**, *3*, 407.
(32) Zhao, Q.; Harris, T. D.; Betley, T. A. *J. Am. Chem. Soc.* **2011**, *133*, 8293.
(33) Eames, E. V.; Betley, T. A. *Inorg. Chem.* **2012**, *19*, 10274.
(34) Klose, A.; Solari, E.; Ferguson, R.; Floriani, C.; Chiesi-Villa, A.; Rizzoli, C.; Re, N. *J. Am. Chem. Soc.* **1994**, *116*, 9123.
(35) Mader, E. A.; Davidson, E. R.; Mayer, J. M. *J. Am. Chem. Soc.* **2007**, *129*, 5153.
(36) Verma, A. K.; Nazif, T. N.; Achim, C.; Lee, S. C. *J. Am. Chem. Soc.* **2000**, *122*, 11013.
(37) Verma, A. K.; Lee, S. C. *J. Am. Chem. Soc.* **1999**, *121*, 10838.
(38) Smith, J. M.; Lachicotte, R. J.; Holland, P. L. *J. Am. Chem. Soc.* **2003**, *125*, 15752.
(39) Vela, J.; Stoian, S.; Flaschenriem, C. J.; Münck, E.; Holland, P. L. *J. Chem. Soc.* **2004**, *126*, 4522.
(40) Ohki, Y.; Takikawa, Y.; Hatanaka, T.; Tatsumi, K. *Organometallics* **2006**, *25*, 311.
(41) Yu, Y.; Brennessel, W. W.; Holland, P. L. *Organometallics* **2007**, *26*, 3217.
(42) Chen, Y.; Zhou, Y.; Chen, P.; Tao, Y.; Li, Y.; Qu, J. *J. Am. Chem. Soc.* **2008**, *130*, 15250.
(43) Zdilla, M. J.; Verma, A. K.; Lee, S. C. *Inorg. Chem.* **2011**, *50*, 1551.
(44) Wucherer, E. J.; Tasi, M.; Hansert, B.; Powell, A. K.; Garland, M.-T.; Halet, J.-F.; Saillard, J.-Y.; Vahrenkamp, H. *Inorg. Chem.* **1989**, *28*, 3564.
(45) Sadique, A. R.; Gregory, E. A.; Brennessel, W. W.; Holland, P. L. *J. Am. Chem. Soc.* **2007**, *129*, 8112.
(46) Betley, T. A.; Peters, J. C. *J. Am. Chem. Soc.* **2004**, *126*, 6252.
(47) Vogel, C.; Heinemann, F. W.; Sutter, J.; Anthon, C.; Meyer, K. *Angew. Chem., Int. Ed.* **2008**, *47*, 2681.
(48) Scepaniak, J. J.; Fulton, M. D.; Bontchev, R. P.; Duesler, E. N.; Kirk, M. L.; Smith, J. M. *J. Am. Chem. Soc.* **2008**, *130*, 10515.
(49) Scepaniak, J. J.; Vogel, C. S.; Khusniyarov, M. M.; Heinemann, F. W.; Meyer, K.; Smith, J. M. *Science* **2011**, *331*, 1049.
(50) Bazhenova, T. A.; Shilov, A. E. *Coord. Chem. Rev.* **1995**, *144*, 69.